Case Studies in Thermal Engineering 28 (2021) 101341

Contents lists available at ScienceDirect

Case Studies in Thermal Engineering

journal homepage: www.elsevier.com/locate/csite

Numerical solutions of convective transport on Brinkman-viscoelastic fluid over a bluff body saturated in porous region

S.F.H. Mohd Kanafiah [a,b], A.R.M. Kasim [a,*], S. Mohd Zokri [c], S. Shafie [d]

[a] Centre for Mathematical Sciences, Universiti Malaysia Pahang, Lebuhraya Tun Razak, 26300, Gambang, Kuantan Pahang, Malaysia
[b] Faculty of Computer and Mathematical Sciences, Universiti Teknologi MARA (UiTM) Cawangan Kelantan, Machang, 18500, Malaysia
[c] Faculty of Computer and Mathematical Sciences, Universiti Teknologi MARA (UiTM) Cawangan Terengganu, Kuala Terengganu, 21080, Malaysia
[d] Department of Mathematical Sciences, Faculty of Science, Universiti Teknologi Malaysia, 81310, Johor Bahru, Johor, Malaysia

ARTICLE INFO

Keywords:
Numerical solution
Horizontal circular cylinder
Brinkman fluid
Viscoelastic fluid
Boundary layer

ABSTRACT

Convective is a fundamental mechanism in heat transfer analysis. Convective heat transport refers to the transfer of heat from one stage to another. In order to produce the preferred output, it is critical to understand the properties of fluid flow. In this study, mixed convection flow is considered, which is defined as a situation where the forces of pressure and buoyancy interact. The goal of this endeavor is to scrutinize the numerical solution of Brinkman-viscoelastic fluid for mixed convection transport over a horizontal circular cylinder as one of the bluff body geometry. Using the necessary similarity transformation, the governing equations were converted into a less complicated form and numerically solved using Keller-box procedure. The influence of mixed convection, Brinkman and viscoelastic parameters towards the fluid velocity and temperature together with skin friction and heat transfer coefficient is analyzed and demonstrated in graphs and tables. This study has revealed that the distribution of fluid velocity, skin friction and heat transfer coefficient had strengthened due to rising values of mixed convection parameter and declined by virtue of increasing viscoelastic and Brinkman parameters. The temperature profile, on the other hand, clearly demonstrates the increasing trend as the Brinkman and viscoelastic parameter increase and declines because of mixed convection. The results show that all of the significant parameters in this investigation affluence the fluid flow characteristics. The provided theoretical results will develop a thorough understanding on boundary layer issues and will be used as a reference for future research or validation.

1. Introduction

People are interested in monitoring the flow behaviour of fluids in engineering applications to satisfy various specifications, such as preserving fluid characteristics over a wide temperature and stress range. Fluid is a substance that flows as a result of shear stress and is classified to type Newtonian and non-Newtonian fluid. The liquid having substance whose shear stress is determined solely by the shear rate and not by yield is called Newtonian type [1]. Meanwhile, non-Newtonian fluid, on the other hand, is caused by changes in viscosity as shear stress is applied to the fluid and may cause rotation and shrinkage [2].

* Corresponding author.
E-mail address: rahmanmohd@ump.edu.my (A.R.M. Kasim).

https://doi.org/10.1016/j.csite.2021.101341
Received 14 June 2021; Received in revised form 5 August 2021; Accepted 11 August 2021
Available online 24 August 2021

Because of potential applications in industries such as oil exploration, construction equipment, cosmetic products, and blood flow, the study of convective transport of heat in fluid flow has received special attention. According to Incropera et al. [3], Convection occurs when a fluid moves from one level to another while being at different temperatures.

Convective heat transfer involving type of non-Newtonian fluid embedded in porosity condition has piqued the attention of many scholars, as has the growing challenge in technology and engineering application. The porous condition is declared for solid phase with void pores or holes, such as building elements, cloth sponges, and human lungs. The Brinkman model is a traditional porous medium model that is applicable for high porosity incompressible fluid flow. Brinkman [4] pioneering work resulted in a model that can be applied to large holey surfaces. Using the Navier Stoke formula, he investigated fluid flow caused by viscous force on the surface of a dense swarm of small spheres. Furthermore, Ali et al. [5] used a new exact solution based on the Laplace transform for the movement of a Brinkman fluid caused by an infinite rotating plate. Following that, Ali et al. [6] investigated the impact of thermally radiation natural convection flows on the unsteady magnetohydrodynamics of Brinkman fluid incorporated with Newtonian heating over a vertical plate. The distribution of fluid velocity and temperature was significantly improved as the Newtonian heating and radiation parameters were increased. Ali et al. [7] then investigated the performance of chemical reactions on Brinkman fluid flow. They investigated how heat and mass diffusion interact with time fractional over an oscillating plate, and used the Laplace transform method to solve both problems.

Khan et al. [8] deliberated the flow of unsteady magnetohydrodynamic for Brinkman flow passing on infinite plate embedded by shear stress that accelerating at the bottom plate. The Fourier as well as finite Fourier transform procedures were used to obtain the solutions. Furthermore, Khan et al. [9] investigated the effect of heat dissipation, chemical reactions, thermal radiation and magnetohydrodynamics on Brinkman fluid across a perpendicular plate. Dubey and Murthy [10] probed the onset of double-diffusive convection towards horizontal through flow while taking convective boundary conditions into account in a porous medium. Apart from that, Kausar et al. [11] focused on the Brinkman flow with frictional heating and porous dissipation over a stretching sheet. Recently, Yadav [12] investigated the onset of convection for Darcy-Brinkman fluid and discovered that Darcy number and gravitational forces were delayed at the start of convection.

The mixed convection flow has sparked a lot of attention in the last few decades because of its potential in industrial applications such as nuclear power plants cooled in an emergency shutdown, solar receivers exposed to power voltage and electronic gadgets cooled by fans. Mixed convection is the combination of free and forced convections act simultaneously at different temperature. There have been many researches on mixed convective boundary layer issues dealing with viscosity and elasticity properties. Kasim et al. [13]

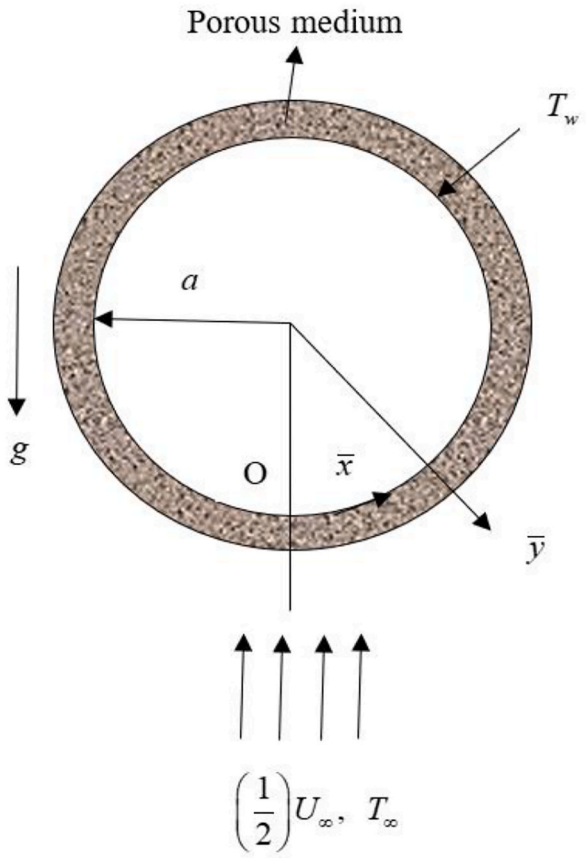

Fig. 1. Physical geometry of model.

examined the heat generation characteristic on viscoelastic fluid passing through a horizontally circular cylinder under condition at boundary as constant heat flux. They demonstrated how the viscoelastic parameter, heat generation, and Prandtl number affected the movement and heat transfer characteristics. Further, Kasim et al. [14] debated on the problem of mixed convection for viscoelastic fluid towards a sphere with magnetic field effect and Newtonian heating in a different work. Meanwhile, Kasim et al. [15] continued the research under the convective boundary condition, ignoring the magnetic field effect. Aziz et al. [16] investigated the outcome of present aligned magnetohydrodynamics on viscoelastic fluid with Newtonian heating over a circular cylinder. Aziz et al. [17] concentrated on the development of a viscoelastic micropolar model in response to a similar problem. Jafar et al. [18] deliberated the performance on viscous dissipation towards viscoelastic fluid flow under geometry of nonlinear stretching sheet. Many researchers have also accentuated the importance of detailed investigations of the fluid behaviors, as shown in Refs. [19–33].

Keeping in view by the preceding literature, the Brinkman model is suitable for the convective boundary layer flow issues in porous medium. The extension and modification of the model by considering another type of fluid could improve the fluid's characteristic. Research has shown that the viscoelastic model that deals with viscosity and elasticity characteristics has gained considerable importance because of its applications in various branches of science and technology. However, there is a limited theoretical analysis on the Brinkman-viscoelastic model. Therefore, the Brinkman concept are used in conjunction with viscoelastic knowledge in this recent study. The problems of mixed convective flow of Brinkman-viscoelastic fluids moving along a horizontal circular cylinder saturated in porous region would be addressed in details. The Keller-box method is used to solve the numerical approach of a nonlinear system. The study focuses on the variations of important parameters such as mixed convection, viscoelastic, and Brinkman parameters over sheer stress and heat transfer characteristics.

2. Problem formulation

A Brinkman-viscoelastic fluid flow for steady mixed convection is generated due to a horizontal circular cylinder with radius, a saturated in porous region. In Cartesian coordinates, $\bar{x}$ is considered along the cylinder and $\bar{y}$ is stately normal to the cylinder surface. The free stream velocity, $^1\!/\!_2 U_\infty$ is moving upward over the cylinder. Let T_w be the constant temperature and T_∞ be atmosphere temperature. The pattern of fluid flow is depicted in Fig. 1.

Using the Boussinesq and boundary layer assumptions, the following fluid model is introduced as

$$\frac{\partial \bar{u}}{\partial \bar{x}}+\frac{\partial \bar{v}}{\partial \bar{y}}=0, \tag{1}$$

$$\begin{aligned}\frac{\mu}{K}\bar{u} = &-\frac{\partial p}{\partial \bar{x}}+\frac{\mu}{\varphi}\left(\frac{\partial^2 \bar{u}}{\partial \bar{x}^2}+\frac{\partial^2 \bar{u}}{\partial \bar{y}^2}\right)\\ &+k_0\left[\begin{array}{l}\bar{u}\left(\frac{\partial^3 \bar{u}}{\partial \bar{x}^3}+\frac{\partial^3 \bar{u}}{\partial \bar{x}\partial \bar{y}^2}\right)+\bar{v}\left(\frac{\partial^3 \bar{u}}{\partial \bar{x}^2\partial \bar{y}}+\frac{\partial^3 \bar{u}}{\partial \bar{y}^3}\right)-\frac{\partial \bar{u}}{\partial \bar{y}}\left(\frac{\partial^2 \bar{u}}{\partial \bar{x}\partial \bar{y}}+\frac{\partial^2 \bar{v}}{\partial \bar{x}^2}\right)\\ +\frac{\partial \bar{u}}{\partial \bar{x}}\left(3\frac{\partial^2 \bar{v}}{\partial \bar{x}\partial \bar{y}}+\frac{\partial^2 \bar{u}}{\partial \bar{y}^2}\right)-2\frac{\partial \bar{v}}{\partial \bar{x}}\frac{\partial^2 \bar{u}}{\partial \bar{x}\partial \bar{y}}\end{array}\right]-\rho g\sin(\bar{x}/a),\end{aligned} \tag{2}$$

$$\bar{u}\frac{\partial T}{\partial \bar{x}}+\bar{v}\frac{\partial T}{\partial \bar{y}}=\alpha_m\left(\frac{\partial^2 T}{\partial \bar{x}^2}+\frac{\partial^2 T}{\partial \bar{y}^2}\right). \tag{3}$$

where $\rho=\rho_\infty[1-\beta(T-T_\infty)]$.

Note that Eqs. (1)–(3) have been adopted by Refs. [17,35]. The velocity of $\bar{x}$ and $\bar{y}$ directions are indicated as $\bar{u}$ and $\bar{v}$, respectively. Besides, μ, K, φ, k_0, ρ, g, p, β, T and α_m are the respective dynamic viscosity, permeability of porous medium, viscoelasticity, fluid density, gravity acceleration, pressure, thermal expansion coefficient, fluid temperature and porous effective thermal diffusivity. The external velocity is defined as

$$\bar{u}_e(\bar{x})=U_\infty\sin(\bar{x}/a)$$

The referred boundary conditions are as follows

$$\begin{aligned}&\bar{v}=0,\quad \bar{u}=0,\quad T=T_w,\quad \text{at}\quad \bar{y}=0,\\ &\bar{u}\to\bar{u}_e(\bar{x}),\quad \bar{v}\to 0,\quad T\to T_\infty\quad \text{as}\quad \bar{y}\to\infty.\end{aligned} \tag{4}$$

The non-dimensional variables are adopted from Ref. [35] to partial removal of physical dimensions from an equation involving physical quantities whereby the less complex equations will be attained.

$$\begin{aligned}&x=\bar{x}/a,\quad y=Pe^{1/2}(\bar{y}/a),\quad u=\bar{u}/U_\infty,\quad v=Pe^{1/2}(\bar{v}/U_\infty),\\ &\theta=(T-T_\infty)/(T_w-T_\infty),\quad u_e(\bar{x})=\bar{u}_e(\bar{x})/U_\infty,\end{aligned} \tag{5}$$

where $Pe=U_\infty a/\alpha_m$ is a revised Péclet number in porous condition. By substituting Eq. (5) into Eqs. (1)–(4), the system is converted to

$$\frac{\partial u}{\partial x}+\frac{\partial v}{\partial y}=0, \tag{6}$$

$$\frac{\partial u}{\partial y}=\Gamma\frac{\partial^3 u}{\partial y^3}+k_1\left[\begin{array}{l} u\dfrac{\partial^4 u}{\partial x\partial y^3}+\dfrac{\partial^3 u}{\partial x\partial y^2}\dfrac{\partial u}{\partial y}+v\dfrac{\partial^4 u}{\partial y^4}+\dfrac{\partial^3 u}{\partial y^3}\dfrac{\partial v}{\partial y}-\dfrac{\partial u}{\partial y}\dfrac{\partial^3 u}{\partial x\partial y^2} \\ -\dfrac{\partial^2 u}{\partial x\partial y}\dfrac{\partial^2 u}{\partial y^2}+\dfrac{\partial u}{\partial x}\dfrac{\partial^3 u}{\partial y^3}+\dfrac{\partial^2 u}{\partial y^2}\dfrac{\partial^2 u}{\partial x\partial y} \end{array}\right]+\lambda\frac{\partial\theta}{\partial y}\sin x, \tag{7}$$

$$u\frac{\partial\theta}{\partial x}+v\frac{\partial\theta}{\partial y}=\frac{\partial^2\theta}{\partial y^2} \tag{8}$$

$$\begin{array}{l} u=0, \quad v=0, \quad \theta=1 \ \ at \ \ \bar{y}=0 \\ u\to u_e, \quad v\to 0, \quad \theta\to 0 \ \ as \bar{y}\to\infty \end{array} \tag{9}$$

Eqs. (6)–(9) are reduced to dimensionless forms by using the following non-similarity transformation variables:

$$\psi=xf(x,y), \quad \theta=\theta(x,y), \tag{10}$$

where ψ implies the stream function demarcated as $u=\frac{\partial\psi}{\partial y}$ and $v=-\frac{\partial\psi}{\partial x}$ for which Eq. (6) is completely fulfilled. Subsequently, Eqs. (7)–(9) lead to

$$\begin{array}{l} f'-\Gamma f'''-k_1\left[2f'f'''-ff^{(iv)}-(f'')^2\right]-(1+\lambda\theta)\dfrac{\sin x}{x}= \\ xk_1\left[f'\dfrac{\partial f'''}{\partial x}-\dfrac{\partial f}{\partial x}f^{(iv)}-f''\dfrac{\partial f''^2}{\partial x}+\dfrac{\partial f'}{\partial x}f'''\right] \end{array} \tag{11}$$

$$\theta''+f\theta'=x\left(f'\frac{\partial\theta}{\partial x}-\frac{\partial f}{\partial x}\theta'\right). \tag{12}$$

$$\begin{array}{l} f(0)=0, \quad f'(0)=0, \quad \theta(0)=1, \qquad \text{at } y=0, \\ f'(\infty)\to\dfrac{\sin x}{x}, \quad f''(\infty)\to 0, \quad \theta(\infty)\to 0 \quad \text{as } y\to\infty. \end{array} \tag{13}$$

Here, $(')$ is corresponds to the derivation with respect toy. Subsequently, the parameters involved in Eq. (11) are defined as $\Gamma=\frac{Da}{\varphi}Pe$ is Brinkman parameter,$\lambda=\frac{Ra}{Pe}$ is mixed convection parameter and $k_1=\frac{k_0KU_\infty Pe}{\mu a^3}$ is viscoelastic parameter. Here, the dimensionless variables are defined as $Da=\frac{K}{a^2}$ is Darcy number and $Ra=\frac{gK\beta(T_w-T_\infty)a}{\alpha_m\nu}$ is Rayleigh number.

At the circular cylinder's lowest stagnation point ($x\approx 0$) Eqs. (11)–(13) are reduced to the form of ordinary differential equations

$$f'-\Gamma f'''-k_1\left[2f'f'''-ff^{(iv)}-(f'')^2\right]-1-\lambda\theta=0, \tag{14}$$

$$\theta''+f\theta'=0. \tag{15}$$

subjected to boundary condition

$$\begin{array}{l} f(0)=0, \quad f'(0)=0, \quad \theta(0)=1 \\ f'(\infty)\to 1, \quad f''(\infty)\to 0, \quad \theta(\infty)\to 0 \end{array} \tag{16}$$

The local skin friction and Nusselt number coefficient are declared as

$$C_f\mathrm{Pr}Pe^{1/2}=x\frac{\partial^2 f}{\partial y^2}, \qquad NuPe^{-1/2}=-\frac{\partial\theta}{\partial y}. \tag{17}$$

3. Solution procedures

The Keller-box technique is applied to equations (11)–(13) as this method

i. Offers unconditional stability and speedy convergence for strongly non-linear flows.
ii. Suitable and appropriate for boundary layer flow equations which are parabolic in nature.
iii. Is one of the most widely applied computational methods in solving any order type problem
iv. Frequently used method for solving boundary layer equations in fluid mechanics.

The first step is to convert the dependent variables into a first order system, as shown below

$$f' = u, u' = v, v' = p, s' = t \tag{18}$$

Eqs. (11) and (12) are then written as

$$u - \Gamma p - k_1\left[2up - fp' - v^2\right] - (1+\lambda s)\frac{\sin x}{x} = xk_1\left[u\frac{\partial p}{\partial x} - \frac{\partial f}{\partial x}p' - v\frac{\partial v}{\partial x} + \frac{\partial u}{\partial x}p\right], \tag{19}$$

$$t' + ft = x\left(u\frac{\partial s}{\partial x} - \frac{\partial f}{\partial x}t\right). \tag{20}$$

and the boundary conditions (13) becomes

$$\begin{aligned} &u = 0, \quad f = 0, \quad s = 1, && \text{at } y = 0, \\ &u \to \frac{\sin x}{x}, \quad v \to 0, \quad s \to 0 && \text{as } y \to \infty. \end{aligned} \tag{21}$$

The central differences are used to transform the first order system into finite difference equations. The mesh points are defined as

$$\begin{aligned} &x^0 = 0, \quad x^n = x^{n-1} + k_n, \quad n = 1, 2, \ldots, N, \\ &y^0 = 0, \quad y_j = y_{j-1} + h_j, \quad j = 1, 2, \ldots, J, \quad y_j \equiv y_\infty. \end{aligned} \tag{22}$$

where k_n is the Δx-spacing and h_j is the Δy-spacing. Note that n and j are the numerical sequence indicating the coordinate location. Fig. 2 displays the net rectangle in the $x - y$ plane.

At any points, the finite difference forms

$$x^{n-1/2} = \frac{1}{2}\left(x^n + x^{n-1}\right), \quad y_{j-1/2} = \frac{1}{2}\left(y_j + y_{j-1}\right), \tag{23}$$

$$()_j^{n-1/2} = \frac{1}{2}\left[()_j^n + ()_j^{n-1}\right], \quad ()_{j-1/2}^n = \frac{1}{2}\left[()_j^n + ()_{j-1}^n\right]. \tag{24}$$

The derivatives in x and y direction for any net function is written as

$$\frac{\partial()}{\partial x} = \frac{()^n - ()^{n-1}}{k_n}, \quad \frac{\partial()}{\partial y} = \frac{()_j - ()_{j-1}}{h_j}. \tag{25}$$

Eqs. (18)-(20) are approximated using centered-difference derivatives at the midpoint $(x^n, y_{j-1/2})$ of the segment P_1P_2 and the corresponding set are

$$f_j - f_{j-1} - \frac{h_j}{2}\left(u_j + u_{j-1}\right) = 0, \tag{26}$$

$$u_j - u_{j-1} - \frac{h_j}{2}\left(v_j + v_{j-1}\right) = 0, \tag{27}$$

$$v_j - v_{j-1} - \frac{h_j}{2}\left(p_j + p_{j-1}\right) = 0, \tag{28}$$

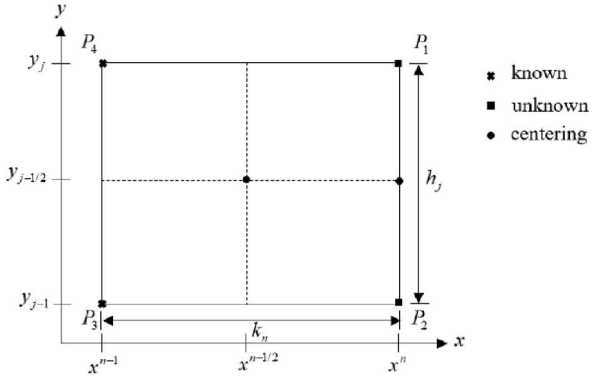

Fig. 2. Net rectangle for $x - y$ plane.

$$s_j - s_{j-1} - \frac{h_j}{2}\left(t_j + t_{j-1}\right) = 0, \tag{29}$$

$$\begin{aligned} &\frac{1}{2}h_j\left(u_j + u_{j-1}\right) - \frac{1}{2}\Gamma h_j\left(p_j + p_{j-1}\right) \\ &-(1+\alpha)\frac{h_j k_1}{2}\left(u_j + u_{j-1}\right)\left(p_j + p_{j-1}\right) + (1+\alpha)\frac{k_1}{2}\left(f_j + f_{j-1}\right)\left(p_j - p_{j-1}\right) \\ &+(1+\alpha)\frac{1}{4}h_j k_1\left(v_j + v_{j-1}\right)\left(v_j + v_{j-1}\right) - \left(1 + \frac{1}{2}\lambda\left(s_j + s_{j-1}\right)\right)Bh_j \\ &-\alpha k_1\left(p_j - p_{j-1}\right)f_{j-1/2}^{n-1} + \alpha\frac{h_j k_1}{4}\left(p'\right)_{j-1/2}^{n-1}\left(f_j + f_{j-1}\right) = \left(R_1\right)_{j-1/2}^{n-1}, \end{aligned} \tag{30}$$

$$\begin{aligned} &t_j - t_{j-1} + \frac{1+\alpha}{4}h_j\left(f_j + f_{j-1}\right)\left(t_j + t_{j-1}\right) \\ &-\alpha h_j\left(\begin{array}{l} \frac{1}{4}\left(u_j + u_{j-1}\right)\left(s_j + s_{j-1}\right) - \frac{1}{2}\left(u_j + u_{j-1}\right)s_{j-1/2}^{n-1} \\ +\frac{1}{2}\left(s_j + s_{j-1}\right)u_{j-1/2}^{n-1} + \frac{1}{2}\left(t_j + t_{j-1}\right)f_{j-1/2}^{n-1} - \frac{1}{2}\left(f_j + f_{j-1}\right)t_{j-1/2}^{n-1} \end{array}\right) = \left(R_2\right)_{j-1/2}^{n-1}. \end{aligned} \tag{31}$$

for which

$$\left(R_1\right)_{j-1/2}^{n-1} = -\left(\begin{array}{l} h_j u_{j-1/2} - \Gamma h_j p_{j-1/2} - h_j k_1\left(2u_{j-1/2}p_{j-1/2} - f_{j-1/2}\left(p'\right)_{j-1/2} - \left(v^2\right)_{j-1/2}\right) \\ -\left(1 + \lambda s_{j-1/2}\right)Bh_j - \alpha h_j k_1\left(-2u_{j-1/2}p_{j-1/2} + f_{j-1/2}\left(p'\right)_{j-1/2} + \left(v^2\right)_{j-1/2}\right) \end{array}\right)^{n-1}$$

$$\left(R_2\right)_{j-1/2}^{n-1} = -\left(\left(t_j - t_{j-1}\right) + (1-\alpha)\ h_j f_{j-1/2}t_{j-1/2} + \alpha h_j u_{j-1/2}s_{j-1/2}\right)^{n-1}$$

Note that $\left(R_1\right)_{j-1/2}^{n-1}$ and $\left(R_2\right)_{j-1/2}^{n-1}$ are the only known quantities. Eqs. (26)-(31) are imposed for each $j = 1, 2, \ldots J$ at the provided n and the boundary conditions (21) become

$$f_0^n = 0, \quad u_0^n = 0, \quad s_0^n = 1, \quad u_J^n = \frac{\sin x}{x}, \quad v_J^n = 0, \quad s_J^n = 0. \tag{32}$$

Assume that f_j^{n-1}, u_j^{n-1}, v_j^{n-1}, p_j^{n-1}, s_j^{n-1}, t_j^{n-1} are known for each $0 \le j \le J$ and leads to a system of unknown variables (f_j^n, u_j^n, v_j^n, p_j^n, s_j^n, t_j^n), $j = 0, 1, \ldots, J$. Next, Eqs. (26)-(31) are linearized. Newton's method is implemented through the use of the iterates listed below

$$f_j^{(i+1)} = f_j^{(i)} + \delta f_j^{(i)}, u_j^{(i+1)} = u_j^{(i)} + \delta u_j^{(i)}, v_j^{(i+1)} = v_j^{(i)} + \delta v_j^{(i)}, p_j^{(i+1)} = p_j^{(i)} + \delta p_j^{(i)}, s_j^{(i+1)} = s_j^{(i)} + \delta s_j^{(i)}, t_j^{(i+1)} = t_j^{(i)} + \delta t_j^{(i)} \tag{33}$$

The terms of higher order for $\delta f_j^{(i)}, \delta u_j^{(i)}, \delta v_j^{(i)}, \delta s_j^{(i)}, \delta t_j^{(i)}, \delta p_j^{(i)}$ and superscript i are neglected and dropped for the simplification process. Performing some algebraic employments yield

$$\delta f_j - \delta f_{j-1} - \frac{1}{2}h_j\left(\delta u_j + \delta u_{j-1}\right) = \left(r_1\right)_{j-1/2}, \tag{34}$$

$$\delta u_j - \delta u_{j-1} - \frac{1}{2}h_j\left(\delta v_j + \delta v_{j-1}\right) = \left(r_2\right)_{j-1/2}, \tag{35}$$

$$\delta v_j - \delta v_{j-1} - \frac{1}{2}h_j\left(\delta p_j + \delta p_{j-1}\right) = \left(r_3\right)_{j-1/2}, \tag{36}$$

$$\delta s_j - \delta s_{j-1} - \frac{1}{2}h_j\left(\delta t_j + \delta t_{j-1}\right) = \left(r_4\right)_{j-1/2}, \tag{37}$$

$$\begin{aligned} &\left(a_1\right)_j\delta v_j + \left(a_2\right)_j\delta v_{j-1} + \left(a_3\right)_j\delta f_j + \left(a_4\right)_j\delta f_{j-1} + \left(a_5\right)_j\delta u_j + \left(a_6\right)_j\delta u_{j-1} \\ &+\left(a_7\right)_j\delta s_j + \left(a_8\right)_j\delta s_{j-1} + \left(a_9\right)_j\delta p_j + \left(a_{10}\right)_j\delta p_{j-1} = \left(r_5\right)_{j-1/2}, \end{aligned} \tag{38}$$

$$\begin{aligned} &\left(b_1\right)_j\delta t_j + \left(b_2\right)_j\delta t_{j-1} + \left(b_3\right)_j\delta f_j + \left(b_4\right)_j\delta f_{j-1} \\ &+\left(b_5\right)_j\delta u_j + \left(b_6\right)_j\delta u_{j-1} + \left(b_7\right)_j\delta s_j + \left(b_8\right)_j\delta s_{j-1} = \left(r_6\right)_{j-1/2}, \end{aligned} \tag{39}$$

where

$$
\begin{aligned}
&(a_1)_j = (1+\alpha)h_j k_1 v_{j-1/2}, && (a_2)_j = (a_1)_j,\\
&(a_3)_j = \frac{(1+\alpha)}{2}k_1\left(p_j - p_{j-1}\right) + \frac{\alpha}{2}h_j k_1 (p')^{n-1}_{j-1/2}, && (a_4)_j = (a_3)_j,\\
&(a_5)_j = \frac{1}{2}h_j - (1+\alpha)h_j k_1 p_{j-1/2}, && (a_6)_j = (a_5)_j,\\
&(a_7)_j = -\frac{1}{2}\lambda B h_j, && (a_8)_j = (a_7)_j,\\
&(a_9)_j = -\frac{1}{2}\Gamma h_j - (1+\alpha)h_j k_1 u_{j-1/2} + (1+\alpha)k_1 f_{j-1/2} - \alpha k_1 f^{n-1}_{j-1/2},\\
&(a_{10})_j = -\frac{1}{2}\Gamma h_j - (1+\alpha)h_j k_1 u_{j-1/2} - (1+\alpha)k_1 f_{j-1/2} + \alpha k_1 f^{n-1}_{j-1/2},
\end{aligned}
\tag{40}
$$

$$
\begin{aligned}
&(b_1)_j = 1 + \frac{(1+\alpha)}{2}h_j f_{j-1/2} - \frac{1}{2}\alpha h_j f^{n-1}_{j-1/2}, \quad (b_2)_j = (b_1)_j - 2,\\
&(b_3)_j = \frac{(1+\alpha)}{2}h_j t_{j-1/2} + \frac{1}{2}\alpha h_j t^{n-1}_{j-1/2}, \qquad (b_4)_j = (b_3)_j\\
&(b_5)_j = -\frac{1}{2}\alpha h_j s_{j-1/2} + \frac{1}{2}\alpha h_j s^{n-1}_{j-1/2}, \qquad (b_6)_j = (b_5)_j\\
&(b_7)_j = -\frac{1}{2}\alpha h_j u_{j-1/2} - \frac{1}{2}\alpha h_j u^{n-1}_{j-1/2}, \qquad (b_8)_j = (b_7)_j
\end{aligned}
\tag{41}
$$

$$
\begin{aligned}
(r_1)_{j-1/2} &= f_{j-1} - f_j + h_j u_{j-1/2},\\
(r_2)_{j-1/2} &= u_{j-1} - u_j + h_j v_{j-1/2},\\
(r_3)_{j-1/2} &= v_{j-1} - v_j + h_j p_{j-1/2},\\
(r_4)_{j-1/2} &= s_{j-1} - s_j + h_j t_{j-1/2},\\
(r_5)_{j-1/2} &= -h_j u_{j-1/2} + \Gamma h_j p_{j-1/2} + 2(1+\alpha)h_j k_1 u_{j-1/2} p_{j-1/2} - (1+\alpha)k_1 f_{j-1/2}\left(p_j - p_{j-1}\right)\\
&\quad -(1+\alpha)h_j k_1 v^2{}_{j-1/2} + Bh_j + \lambda B h_j s_{j-1/2} + \alpha k_1\left(p_j - p_{j-1}\right) f^{n-1}_{j-1/2}\\
&\quad -\alpha h_j k_1 f_{j-1/2}(p')^{n-1}_{j-1/2} + (R_1)^{n-1}_{j-1/2},\\
(r_6)_{j-1/2} &= -t_j + t_{j-1} - (1+\alpha)h_j f_{j-1/2} t_{j-1/2} + \alpha h_j \begin{pmatrix} u_{j-1/2}s_{j-1/2} - u_{j-1/2}s^{n-1}_{j-1/2} + s_{j-1/2}u^{n-1}_{j-1/2}\\ +t_{j-1/2}f^{n-1}_{j-1/2} - f_{j-1/2}t^{n-1}_{j-1/2}\end{pmatrix} + (R_2)^{n-1}_{j-1/2}
\end{aligned}
\tag{42}
$$

The following boundary conditions are assumed in all iterates in order to maintain the correct values

$$\delta f^n_0 = 0,\ \delta u^n_0 = 0,\ \delta s^n_0 = 0,\ \delta u^n_J = 0,\quad \delta v^n_J = 0,\quad \delta s^n_J = 0 \tag{43}$$

Lastly, the above linear tridiagonal systems from Eqs. (34)–(39) can be fixed using block tridiagonal elimination procedure. Writing the equations as in the block matrix form

$$[A][\delta] = [r], \tag{44}$$

where

$$
\begin{bmatrix}
[A_1] & [C_1] & & & & & \\
[B_2] & [A_2] & [C_2] & & & & \\
 & \ddots & \ddots & \ddots & & & \\
 & & & [B_{J-1}] & [A_{J-1}] & [C_{J-1}] & \\
 & & & & [B_J] & [A_J] &
\end{bmatrix}
\begin{bmatrix} [\delta_1] \\ [\delta_2] \\ \vdots \\ \vdots \\ \vdots \\ [\delta_{J-1}] \\ [\delta_J] \end{bmatrix}
=
\begin{bmatrix} [r_1] \\ [r_2] \\ \vdots \\ \vdots \\ \vdots \\ [r_{J-1}] \\ [r_J] \end{bmatrix}.
$$

The given elements of the matrices are

$$
[A_1] = \begin{bmatrix}
0 & 0 & 0 & 1 & 0 & 0 \\
d_1 & 0 & 0 & 0 & 0 & 0 \\
-1 & d_1 & 0 & 0 & d_1 & 0 \\
0 & 0 & d_1 & 0 & 0 & d_1 \\
(a_2)_1 & (a_{10})_1 & 0 & (a_3)_1 & (a_9)_1 & 0 \\
0 & 0 & (b_2)_1 & (b_3)_1 & 0 & (b_1)_1
\end{bmatrix}
\tag{45}
$$

$$[A_j] = \begin{bmatrix} d_j & 0 & 0 & 1 & 0 & 0 \\ -1 & d_j & 0 & 0 & 0 & 0 \\ 0 & -1 & 0 & 0 & d_j & 0 \\ 0 & 0 & -1 & 0 & 0 & d_j \\ (a_6)_j & (a_2)_j & (a_8)_j & (a_3)_j & (a_9)_j & 0 \\ (b_6)_j & 0 & (b_8)_j & (b_3)_j & 0 & (b_1)_j \end{bmatrix}, 2 \le j \le J, \tag{46}$$

$$[B_j] = \begin{bmatrix} 0 & 0 & 0 & -1 & 0 & 0 \\ 0 & 0 & 0 & 0 & 0 & 0 \\ 0 & 0 & 0 & 0 & d_j & 0 \\ 0 & 0 & 0 & 0 & 0 & d_j \\ 0 & 0 & 0 & (a_4)_j & (a_{10})_j & 0 \\ 0 & 0 & 0 & (b_4)_j & 0 & (b_2)_j \end{bmatrix}, 2 \le j \le J, \tag{47}$$

$$[C_j] = \begin{bmatrix} d_j & 0 & 0 & 0 & 0 & 0 \\ 1 & d_j & 0 & 0 & 0 & 0 \\ 0 & 1 & 0 & 0 & 0 & 0 \\ 0 & 0 & 1 & 0 & 0 & 0 \\ (a_5)_j & (a_1)_j & (a_7)_j & 0 & 0 & 0 \\ (b_5)_j & 0 & (b_7)_j & 0 & 0 & 0 \end{bmatrix}, 1 \le j \le J-1 \tag{48}$$

$$[\delta_1] = \begin{bmatrix} \delta v_0 \\ \delta p_0 \\ \delta t_0 \\ \delta f_1 \\ \delta p_1 \\ \delta t_1 \end{bmatrix}, [\delta_j] = \begin{bmatrix} \delta u_{j-1} \\ \delta v_{j-1} \\ \delta s_{j-1} \\ \delta f_j \\ \delta p_j \\ \delta t_j \end{bmatrix}, 2 \le j \le J \tag{49}$$

and

$$[r_j] = \begin{bmatrix} (r_1)_{j-1/2} \\ (r_2)_{j-1/2} \\ (r_3)_{j-1/2} \\ (r_4)_{j-1/2} \\ (r_5)_{j-1/2} \\ (r_6)_{j-1/2} \end{bmatrix}, 1 \le j \le J. \tag{50}$$

The matrix A is assumed as nonsingular and Eq. (44) can be considered as

$$[A] = [L][U],$$

$$= \begin{bmatrix} [\alpha_1] & & & & \\ [B_2] & [\alpha_2] & & & \\ & \ddots & \ddots & & \\ & & & [\alpha_{J-1}] & \\ & & & [B_J] & [\alpha_J] \end{bmatrix} \begin{bmatrix} [I] & [\Gamma_1] & & & \\ & [I] & [\Gamma_2] & & \\ & & \ddots & \ddots & \\ & & & [I] & [\Gamma_{J-1}] \\ & & & & [I] \end{bmatrix} \tag{51}$$

where $[I]$ is the matrix identically of size 6, $[\alpha_i]$ and $[\Gamma_i]$ are 6×6 matrices in which components of the matrices are defined as

$$[\alpha_1] = [A_1], \tag{52}$$

$$[A_1] \quad [\Gamma_1] = [C_1], \tag{53}$$

$$[\alpha_j] = [A_j] - [B_j] \quad [\Gamma_{j-1}], j = 2,\ 3,\ \ldots,\ J \tag{54}$$

$$[\alpha_j]\,[\Gamma_j] = [C_j], j = 2,\ 3,\ \ldots,\ J-1. \tag{55}$$

When Eq. (51) is substituted into Eq. (44), the results is

$$[L][U][\delta] = [r]. \tag{56}$$

By defining

$$[U][\delta] = [W], \tag{57}$$

Thus, Eq. (56) yield

$$[L][W] = [r], \tag{58}$$

where

$$W = \begin{bmatrix} [W_1] \\ [W_2] \\ \vdots \\ [W_{J-1}] \\ [W_J] \end{bmatrix}, \tag{59}$$

and $[W_j]$ are of size 6×1 matrix. The elements of W from Eq. (58) can then be solved as

$$[\alpha_1][W_1] = [r_1], \tag{60}$$

$$[\alpha_j][W_j] = [r_j] - [B_j][W_{j-1}], 2 \le j \le J. \tag{61}$$

The computations of Γ_j, α_j and W_j is commonly known as the forward sweep. After obtaining the entries of W from Eq. (54), the δ is obtained by using a backward sweep. As a result, the following relationships are obtained as

$$[\delta_J] = [W_J], \tag{62}$$

$$[\delta_j] = [W_j] - [\Gamma_j][\delta_{j+1}], 1 \le j \le J-1. \tag{63}$$

These computations are repeated until a convergence condition is met, at which point these are terminated

$$\left|\delta v_0^{(i)}\right| < \varepsilon_1, \tag{64}$$

where $\varepsilon_1 = 10^{-7}$ is a too small fixed value.

4. Solution methodologies

The numerical solution was achieved by applying the Keller-box procedure to Eqs. (11) and (12) with appropriate boundary conditions (13) for a variety of physical variables such as Brinkman Γ, viscoelastic k_1 and mixed convection λ. The boundary layer thickness was chosen within the range of 3–7 to ensure that all numerical solutions reached the boundary conditions asymptotically. MATLAB software was used to build the algorithm. To demonstrate the accuracy of the obtained results, a comparison was made between the current result and a previously published result.

For various value of λ, the fixed parameters of Brinkman and viscoelastic used are $\Gamma = 0.1$ and $k_1 = 0$, except otherwise stated. As shown in Table 1, the existing numerical outputs for skin friction coefficient C_f are compared to those published by Nazar et al. [34] and Tham et al. [35]. The result shows excellent agreement, indicating that the proposed computation is accurate and acceptable.

5. Results and discussion

The skin friction quantity C_f and Nusselt number Nu versus the significant parameter values is shown in Table 2. The skin friction coefficient is noticed to decrease when Γ and k_1 increase, while for increasing λ, the reverse trend is perceived. Meanwhile, the Nusselt number Nu decreases as Γ and k_1 increase and improves by increasing the λ. The decrease in Nusselt number Nu indicates poor heat transfer owing to the dominance of the heat convection effect at the cold cylinder $(\lambda < 0)$.

Figs. 3 and 4 display the output of variance in value of viscoelastic parameter k_1 on fluid velocity $f'(y)$ also temperature $\theta(y)$. It is perceived the increases of k_1, led to decrease the fluid velocity. This indicates that the fluid viscosity has slowed the fluid velocity. The increment of k_1, on the other hand, shows the opposite trend for the temperature profile. This circumstance occurs due to the viscosity and elasticity properties of the fluid. The configuration on the effect of varying λ for fluid velocity and temperature are presented in Figs. 5 and 6. The buoyancy force affects the λ as well. Increasing λ causes the buoyancy forces on the external flow to be induced, resulting in a pressure gradient that helps to slightly increase the fluid velocity while reducing the temperature insignificantly. The heat transfer of cooling effect would then increase, thus lowering the temperature. Figs. 7 and 8 demonstrate the characteristic of fluid velocity and temperature due to the Brinkman factor. These figures show that the increased in Γ values have decreased the velocity due

Table 1
Assessment of skin friction coefficient C_f at $\Gamma = 0.1$ and $k_1 = 0$.

λ	$x = 0.4$		
	Nazar et al. [34]	Tham et al. [35]	Current
−1.13	0.0207	0.0574	0.0211
−1.03	0.1397	0.1404	0.1403
−1.0	0.1745	0.1753	0.1753
0	1.2281	1.2314	1.2314
1	2.1759	2.1814	2.1814
2	3.0673	3.0749	3.0749

Table 2
Numerical values of C_f and Nu for variation of λ, Γ and k_1.

λ	Γ	k_1	C_f	Nu
−0.5	0.1	1.0	0.010348	0.004258
−0.1			0.013997	0.004485
0.5			0.018334	0.004738
1.0			0.021364	0.004905
1.0	1.0	4	0.005599	0.004321
	2.0		0.004997	0.004229
	4.0		0.004251	0.004088
	6.0		0.003783	0.003983
1.0	0.1	4.5	0.012066	0.003715
		5.0	0.011550	0.003659
		6.0	0.010745	0.003539
		8.0	0.009503	0.003377

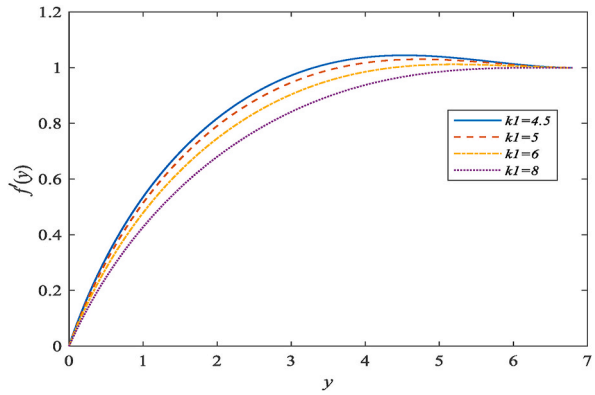

Fig. 3. Performance of k_1 on $f'(y)$.

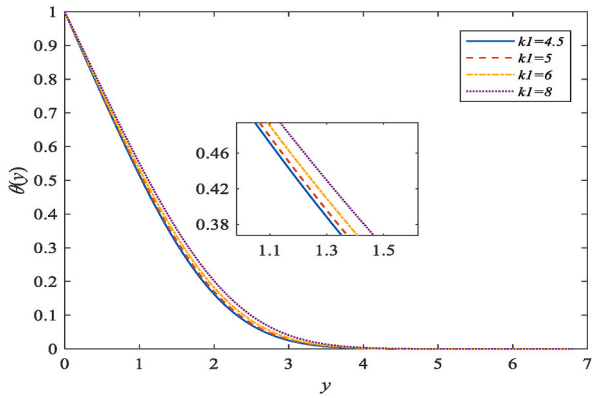

Fig. 4. Performance of k_1 on $\theta(\eta)$.

to increase drag force, while increasing temperature and thermal boundary layer thickness. A high Brinkman parameter value indicates that there is increase in resistance caused by the presence of the solid matrix.

6. Conclusion

The current study generated a numerical result for the Brinkman viscoelastic fluid model through a horizontal circular cylinder saturated in porous region. By implementing the suitable non-dimensional and non-similarity transformation variables, the fluid model is converted into dimensionless form. The numerical solutions of the problem are tackled using the Keller-box approach and Matlab software. To summarize, all of the parameters investigated in this study significantly impact the fluid flow behaviours. Skin friction and heat transfer are both reduced as the Brinkman and viscoelastic parameters are increased, and both are increased as the

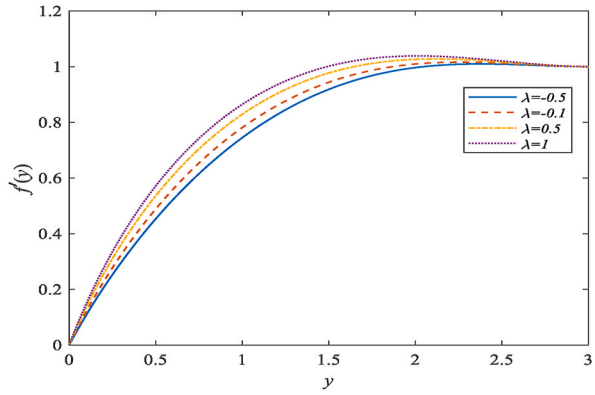

Fig. 5. Performance of λ on $f'(y)$.

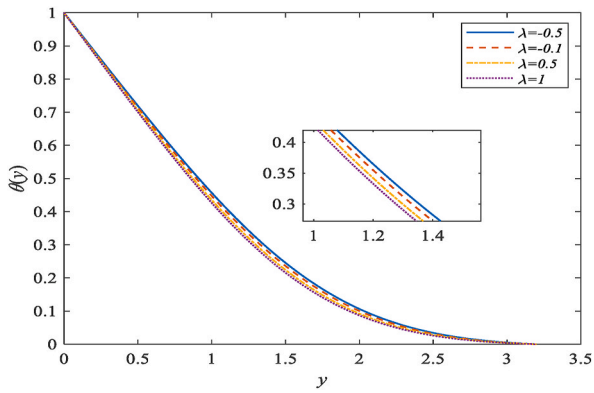

Fig. 6. Performance of λ on $\theta(y)$.

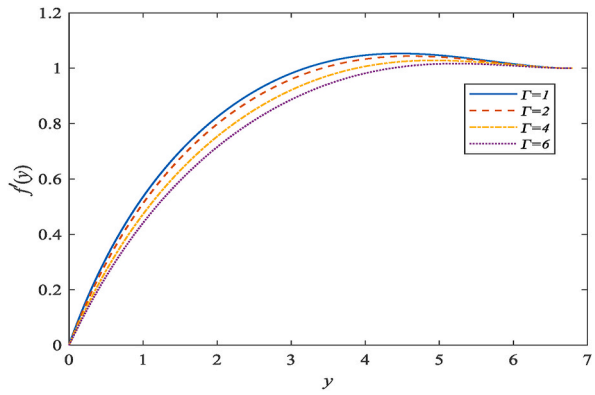

Fig. 7. Performance of Γ on $f'(y)$.

mixed convection parameter is increased. Furthermore, the effect of increasing the mixed convection, Brinkman and viscoelastic parameter on velocity and temperature profiles is contradict. The above mentioned outcomes help the researchers to better understand the phenomenon of fluid flow. Furthermore, the provided comprehensive numerical results will aid in the future solution of computational fluid dynamic problems. The output can also be used as a foundation for complex flow problems.

Funding statement

"This project has been supported by the Ministry of Higher Education and Universiti Malaysia Pahang through RDU192602 & PGRS2003169."

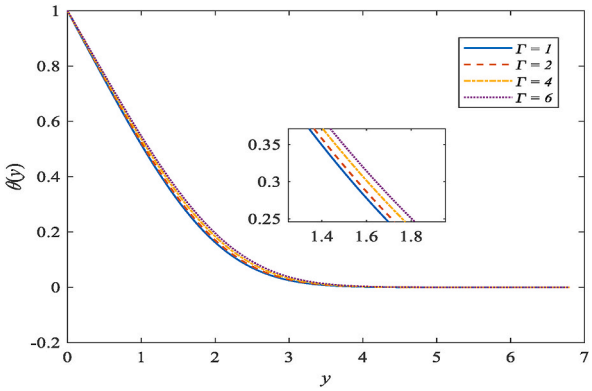

Fig. 8. Performance of Γ on $\theta(y)$.

CRediT authorship contribution statement

S.F.H. Mohd Kanafiah: Writing – original draft, Methodology, Writing – review & editing, Resources. **A.R.M. Kasim:** Methodology, Investigation, Results and discussion, Resources. **S. Mohd Zokri:** Methodology, Writing – review & editing, Resources. **S. Shafie:** Investigation, Results and discussion, Resources.

Declaration of competing interest

The authors declare that they have no known competing financial interests or personal relationships that could have appeared to influence the work reported in this paper.

Acknowledgement

"The authors would like to acknowledge The Ministry of Higher Education Malaysia and Universiti Malaysia Pahang for the financial support through The Fundamental Research Grant Scheme for Research Acculturation of Early Career Researchers (FRGS-RACER) (Ref: RACER/1/2019/STG06/UMP//1) through RDU192602 & PGRS2003169. Deep appreciation also extended to Universiti Teknologi MARA Cawangan Kelantan, Machang Campus for the guidance and support."

References

[1] H. Ghobadi, M.G. Hassankolaei, Numerical treatment of magneto Carreau nanofluid over a stretching sheet considering Joule heating impact and nonlinear thermal ray, Heat Tran. Asian Res. 48 (8) (2019) 4133–4151.
[2] B.R. Jaiswal, A non-Newtonian liquid sphere embedded in a polar fluid saturated porous medium: Stokes flow, Appl. Math. Comput. 316 (2018) 488–503.
[3] F.P. Incropera, D.P. DeWitt, T.L. Berqmanand, A.S. Lavine, Fundamentals of Heat and Mass Transfer, John Wiley and Sons, New York, 2006 [online]. Available, my1lib.org/book/511826/d47a5e.
[4] H.C. Brinkman, On the permeability of media consisting of closely packed porous particles, Appl. Sci. Res. 1 (1) (1949) 81–86.
[5] F. Ali, I. Khan, S.U. Haq, S. Shafie, A note on new exact solutions for some unsteady flows of brinkman-type fluids over a plane wall, Sect. A J. Phys. Sci. 67 (6–7) (2012) 377–380.
[6] F. Ali, I. Khan, S.U. Haq, S. Shafie, Influence of thermal radiation on unsteady free convection mhd flow of brinkman type fluid in a porous medium with Newtonian heating, Math. Probl Eng. (2013) 1–14, 2013.
[7] F. Ali, S.A.A. Jan, I. Khan, M. Gohar, N.A. Sheikh, Solutions with special functions for time fractional free convection flow of Brinkman-type fluid, Eur. Phys. J. Plus 131 (9) (2016) 1–13.
[8] Z.A. Khan, S.U. Haq, T.S. Khan, I. Khan, I. Tlili, Unsteady MHD flow of a Brinkman type fluid between two side walls perpendicular to an infinite plate, Result. Phys. 9 (2018) 1602–1608.
[9] A. Khan, D. Khan, I. Khan, F. Ali, F. Ul Karim, et al., MHD flow of brinkman type H2O-Cu, Ag, TiO2 and Al2O3 nanofluids with chemical reaction and heat generation effects in a porous medium, J. Magn. 24 (2) (2019) 262–270.
[10] R. Dubey, P.V.S.N. Murthy, The onset of double-diffusive convection in a Brinkman porous layer with convective thermal boundary conditions, in: Proc. AIP Advance, New York, NY, USA, 2019, 045322.
[11] M.S. Kausar, A. Hussanan, M. Mamat, B. Ahmad, Boundary layer flow through Darcy-Brinkman porous medium in the presence of slip effects and porous dissipation, Symmetry 11 (5) (2019) 1–11.
[12] D. Yadav, "The onset of Darcy-Brinkman convection in a porous medium layer with vertical throughflow and variable gravity field effects, J. Heat Tran. 49 (5) (2020) 3161–3173.
[13] A.R.M. Kasim, N.F. Mohammad, S. Shafie, I. Pop, Constant heat flux solution for mixed convection boundary layer viscoelastic fluid, J. Heat Mass Transf. 49 (2) (2013) 163–171.
[14] A.R.M. Kasim, N.F. Mohammad, S. Shafie, Mixed convection flow of viscoelastic fluid over a sphere with constant heat flux, in: Proc. AIP, New York, NY, USA, 2013, pp. 453–461.
[15] A.R.M. Kasim, L.Y. Jiann, N.A. Rawi, A. Ali, S. Shafie, Mixed convection flow of viscoelastic fluid over a sphere under convective boundary condition embedded in porous medium, Defect Diffusion Forum 362 (2015) 67–75.
[16] L.A. Aziz, A.R.M. Kasim, H.A.M. Al-sharifi, M.Z. Salleh, N.F. Mohammed, et al., Influence of aligned MHD on convective boundary layer flow of viscoelastic fluid, in: Proc. AIP, New York, NY, USA, 2017, 03005.

[17] L.A. Aziz, A.R.M. Kasim, M.Z. Salleh, Development on mathematical model of convective boundary layer flow of viscoelastic fluid with microrotation effect under constant wall temperature thermal condition over a bluff body, ASM Sci. J. 12 (5) (2019) 86–90.
[18] A.B. Jafar, S. Shafie, I. Ullah, Magnetohydrodynamic boundary layer flow of a viscoelastic fluid past a nonlinear stretching sheet in the presence of viscous dissipation effect, Coatings 9 (8) (2019) 1–20.
[19] H. Ahmad, T. Javed, A. Ghaffari, Radiation effect on mixed convection boundary layer flow of a viscoelastic fluid over a horizontal circular cylinder with constant heat flux, J. Appl. Fluid Mech. 9 (3) (2016) 1167–1174.
[20] P.G. Metri, S. Abel, S. Silvestrov, Heat transfer in MHD mixed convection viscoelastic fluid flow over a stretching sheet embedded in a porous medium with viscous dissipation and non-uniform heat source/sink, Procedia Eng. 157 (2016) 309–316.
[21] S. Eswaramoorthi, M. Bhuvaneswari, S. Sivasankaran, S. Rajan, Effect of radiation on MHD convective flow and heat transfer of a viscoelastic fluid over a stretching surface, Procedia Eng. 127 (2015) 916–923.
[22] S.R. Mishra, R.S. Tripathy, G.C. Dash, MHD viscoelastic fluid flow through porous medium over a stretching sheet in the presence of non-uniform heat source/sink, Rendiconti del Circolo Matematico di Palermo Series 2 (1) (2018) 129–143, 67.
[23] A. Mastroberardino, U.S. Mahabaleswar, Mixed convection in viscoelastic flow due to a stretching sheet in a porous medium, J. Porous Media 16 (6) (2013) 483–500.
[24] R. Mahat, N.A. Rawi, S. Shafie, A.R.M. Kasim, Mixed convection boundary layer flow of viscoelastic nanofluid past a horizontal circular cylinder with convective boundary condition, Int. J. Mech. Eng. Robot. Res. 8 (1) (2019) 87–91.
[25] R. Mahat, N. Afiqah, A.R.M. Kasim, S. Shafie, "Heat generation effect on mixed convection flow of viscoelastic nanofluid : convective boundary condition solution, J. Adv. Res. Micro Nano Eng. 16 (2) (2020) 166–172.
[26] G. Kotha, T. Kannan, P. Jayalakshmi, Magnetohydrodynamic micropolar nanofluid past a permeable stretching/shrinking sheet with Newtonian heating, J. Braz. Soc. Mech. Sci. Eng. 39 (11) (2017) 4379–4391.
[27] G. Kotha, K. Kukkamalla, S.M. Ibrahim, Effect of thermal radiation on engine oil nanofluid flow over a permeable wedge under convective heating: Keller box method, Multidiscip. Model. Mater. Struct. 15 (1) (2018) 187–205.
[28] G. Kotha, V.R. Kolipaula, M.V.S. Rao, S. Penki, A.J. Chamkha, Internal heat generation on bioconvection of an MHD nanofluid flow due to gyrotactic microorganisms, Eur. Phys. J. Plus 135 (7) (2020) 1–19.
[29] M.V.S. Rao, G. Kotha, A.J. Chamkha, et al., Bioconvection in a convectional nanofluid flow containing gyrotactic microorganisms over an isothermal vertical cone embedded in a porous surface with chemical reactive species, Arabian J. Sci. Eng. 46 (2021) 2493–2503.
[30] G. Kotha, R.E. Nayak, M.V.S. Rao, et al., "Nodal/Saddle stagnation point slip flow of an aqueous convectional Magnesium Oxide–Gold hybrid nanofluid with viscous dissipation, Arabian J. Sci. Eng. 46 (2021) 2701–2710.
[31] K.D. Ramaiah, P. Surekha, G. Kotha, K. Thangavelu, Mhd rotating flow of a Maxwell fluid with arrhenius activation energy and non-Fourier heat flux model, Heat Transf. 49 (4) (2020) 2209–2227.
[32] G. Kotha, T. Kannan, G. Sakthivel, K.D. Ramaiah, Unsteady free convective boundary layer flow of a nanofluid past a stretching surface using a spectral relaxation method, Int. J. Ambient Energy 41 (6) (2018) 609–616.
[33] K.V. Ramana, G. Kotha, T. Kannan, et al., "Cattaneo–Christov heat flux theory on transverse MHD Oldroyd-B liquid over nonlinear stretched flow, J. Therm. Anal. Calorim. (2021).
[34] R. Nazar, N. Amin, D. Filip, I. Pop, The Brinkman model for the mixed convection boundary layer flow past a horizontal circular cylinder in a porous medium, Int. J. Heat Mass Tran. 46 (17) (2003) 3167–3178.
[35] L. Tham, R. Nazar, I. Pop, Mixed convection boundary layer flow past a horizontal circular cylinder embedded in a porous medium saturated by a nanofluid: brinkman model, J. Porous Media 16 (5) (2013) 445–457.